Superior tribological properties of an amorphous carbon film with a graphite-like structure*

Wang Yong-Jun(王永军)[a)b)], Li Hong-Xuan(李红轩)[a)], Ji Li(吉 利)[a)], Liu Xiao-Hong(刘晓红)[a)], Wu Yan-Xia(吴艳霞)[a)b)], Zhou Hui-Di(周惠娣)[a)], and Chen Jian-Min(陈建敏)[a)†]

[a)] *State Key Laboratory of Solid Lubrication, Lanzhou Institute of Chemical Physics, Chinese Academy of Sciences, Lanzhou* 730000, *China*

[b)] *Graduate University of the Chinese Academy of Sciences, Beijing* 100049, *China*

(Received 4 March 2011; revised manuscript received 16 August 2011)

Amorphous carbon films with high sp^2 concentrations are deposited by unbalanced magnetron sputtering with a narrow range of substrate bias voltage. Field emission scanning electron microscopes (FESEMs), high resolution transmission electron microscopes (HRTEMs), atomic force microscopes (AFMs), the Raman spectrometers, nano-indentation, and tribometers are subsequently used to characterize the microstructures and the properties of the resulting films. It is found that the present films are dominated by the sp^2 sites. However, the films demonstrate a moderate hardness together with a low internal stress. The high hardness of the deposited film originates from the crosslinking of the sp^2 clusters by the sp^3 sites. The presence of the graphite-like clusters in the film structure may be responsible for the low internal stress. What is more important is that the resulting films show excellent tribological properties with high load capacity and excellent wear resistance in humid atmospheres. The relationship between the microstructure determined by the deposition condition and the film characteristic is discussed in detail.

Keywords: magnetron sputtering, graphite-like carbon film, microstructure, performance

PACS: 61.43.Dq, 62.20.Qp, 68.55.Ln **DOI:** 10.1088/1674-1056/21/1/016101

1. Introduction

Amorphous carbon films have received extensive attention during the past two decades because of their exceptional properties of high mechanical hardness, low friction, and other material properties.[1] However, their practical applications in severe operating conditions, e.g., high load condition, are strongly restricted by the high internal stress of the films, which could lead to the delamination of the films from metal substrates due to the poor adhesion strength between the films and the substrates. Fortunately, recent studies have shown that graphite-like carbon film demonstrates excellent tribological properties in the high load conditions.[2−5] It provides a new perspective for developing the load capacity of carbonaceous materials. However, studies on the characteristics of the graphite-like carbon films, which will be conducible to expanding their applications in high load engineering conditions, is scarce.

Our previous studies have shown that graphite-like carbon films can be successfully prepared by using the unbalanced magnetron sputtering technique.[6] However, it is found that the deposition rate of carbon film is very low owing to the low sputtering yield of graphite targets, which restricts its industrial production. Besides, the doping of the graphite-like carbon film with other elements, e.g. titanium, cannot be effectively achieved by magnetron sputtering with a pair of graphite targets. Thus, the deposition system is improved in this work to be free of the above-mentioned limitations. The main differences between the present work and our previous one lie in the sputtering system, the interlayer, and the substrate.

In this work, the graphite-like carbon films are prepared by medium frequency alternating-current unbalanced magnetron sputtering with a pair of graphite targets and direct-current (DC) unbalanced magnetron sputtering with a graphite target. The microstructures and the properties of the graphite-like carbon films are investigated by using a field emission

*Project supported by the National Natural Science Foundation of China (Grant Nos. 50705093 and 50575217), the Innovative Group Foundation of the National Natural Science Foundation of China (Grant No. 50421502), and the National Basic Research Program of China (Grant No. 2007CB607601).

†Corresponding author. E-mail: Chenjm@licp.cas.cn

© 2012 Chinese Physical Society and IOP Publishing Ltd

scanning electron microscope, a high resolution transmission electron microscope, an atomic force microscope, Raman spectroscopy, nano-indentation, and a tribometer. The influence of the deposition bias voltage on the film's characteristics is discussed in detail.

2. Experimental details

2.1. Film deposition

A series of graphite-like carbon films with thicknesses of about 1000 nm were prepared on silicon substrates by alternating-current unbalanced magnetron sputtering with a pair of graphite targets and direct-current unbalanced magnetron sputtering with a graphite target. Figure 1 shows the schematic diagram of the deposition system, which is composed of a pulsed bias assisted radio frequency (RF) inductively coupled plasma chemical vapour deposition unit, a medium frequency (40 kHz) alternating-current unbalanced magnetron sputtering unit, and a direct-current unbalanced magnetron sputtering unit. There were four sputtering targets in the chamber marked as A, B, C, and D respectively. The A and B targets (graphite) controlled by one medium frequency alternating-current power supply were employed as the carbon source, and C (graphite) and D (titanium) targets each were connected to one direct-current power supply. The C target (graphite) was used as a carbon source too, and the interlayer was obtained from the D target (titanium). A 40 kHz midfrequency unipolar pulsed direct-current power supply was connected to the substrate holder and the sample holder station to control the substrate bias voltage. In the present case, the radio frequency was not used, and the films were deposited only by using the sputtering system. Before the deposition, the samples were cleaned ultrasonically in deionized water, acetone, and alcohol for 20 min sequentially, and then they were placed on the sample holder station, which was rotated to pass through the front of each sputtering target in turn during the deposition so as to enhance the uniformity of the deposited film. After that, the deposition system was heated up to 100 °C, meanwhile a pressure about 10^{-3} Pa was obtained by using a turbomolecular pumping system. Subsequently, the samples were etched with Ar^+ ions in the vacuum chamber under a bias voltage of 600 V at a pressure of 1.6 Pa for 20 min to remove the native oxide layers from the surfaces of the samples.

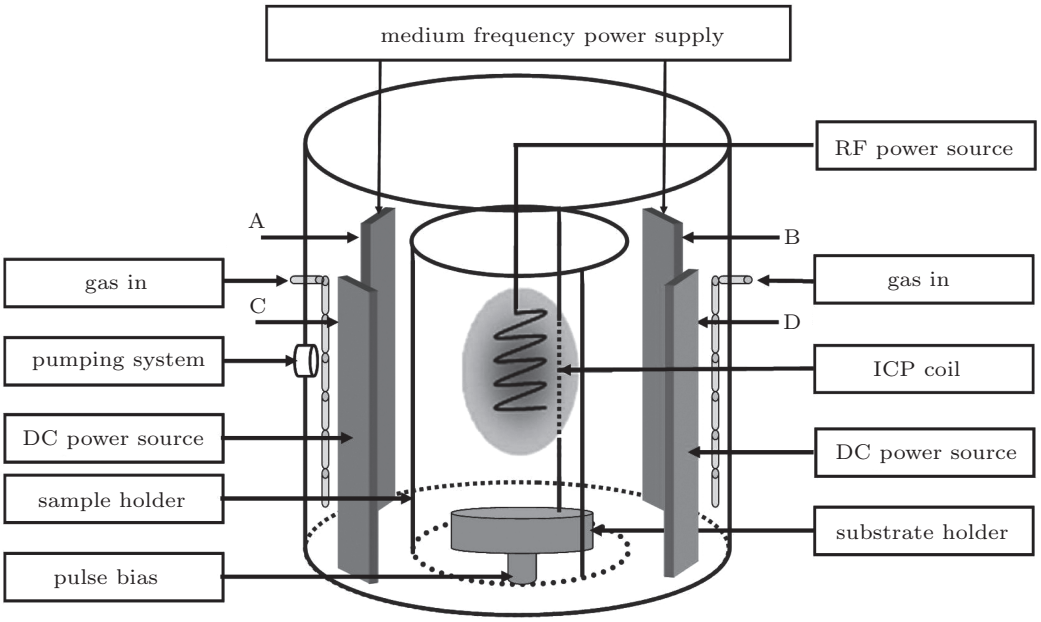


Fig. 1. Schematic diagram of the deposition system.

The main deposition processes were as follows. Firstly, a titanium interlayer with a thickness of about 400 nm was deposited from the D target (titanium) under a working pressure of 0.3 Pa (which is not changed in the next deposition process). Secondly, three graphite targets and one titanium target, which were 15 cm away from the sample holder station, were cosputtered to produce a Ti+C graded interlayer with

a thickness of 200 nm. During this process, the sputtering current of the titanium target decreased gradually to 0 A, and those of the graphite targets increased to 6 A (A and B targets) and 3 A (C target), respectively. Finally, the graphite-like carbon films were deposited on the Ti+C graded interlayer under a duty ratio of 30% at the substrate bias voltages of 75 V, 100 V, 125 V, and 150 V, respectively. The deposition time of the topmost graphite-like carbon film was 3 h.

2.2. Film characterization

The cross-sectional structure of the graphite-like carbon film was observed using a field emission scanning electron microscope (FESEM, JSM-6701F, Japan). The high resolution transmission electron microscope (HRTEM) image of the film was obtained on a JEOL 2010 TEM operated at 200 kV. The sample film with a thickness of about 30 nm for the high resolution transmission electron microscope observation was first deposited on the NaCl substrate followed by the dissolution of the NaCl substrate in distilled water. The surface morphology of the film was observed using a digital instrument nanoscope III and a multimode atomic force microscope (AFM). A LabRAM HR800 micro-Raman spectrometer (HORIBA Jobin Yvon, France) operating with a 532 nm Ar^+ laser as the excitation source was used to characterize the film structure. The Raman spectra were fitted based on two Gaussian shape curves with a curve-fitting software to identify the peak positions. The hardness and the elastic modulus of the films were determined using a NanoTest 600 nanomechanical system (MicroMaterials Ltd, UK), and the maximum indentation depth was controlled to be about 100 nm (less than 10% of the film thickness) to minimize the effect of the substrate. Five repeated indentations were made for each sample.

The curvature radii of the graphite-like carbon films were measured using a MicroXAM surface mapping microscope (ADE shift, US), and the internal stress was calculated by using the Stoney equation[7]

$$\sigma = \frac{E_{\rm s}}{6\,(1-v_{\rm s})}\left(\frac{t_{\rm s}^2}{t_{\rm f}}\right)\left(\frac{1}{R_2}-\frac{1}{R_1}\right),$$

where σ is the internal stress, R_1 and R_2 are the substrate curvature radii before and after the film deposition, $\nu_{\rm s}$ and $E_{\rm s}$ are the Poisson's ratio and the Young's modulus of the substrate, $t_{\rm s}$ and $t_{\rm f}$ are the thicknesses of the substrate and the film, respectively.

The tribological properties of the graphite-like carbon film were measured using a reciprocating-type ball-on-disc tribometer (CSM, Tribo-S-D-0000), which was equipped with an environmental chamber. In the chamber, the relative humidity and the gaseous environment could be controlled. With a relative humidity of 70%, all the tribological tests were preformed at room temperature under a load of 20 N. Steel balls (GCr15, Φ3 mm) and ceramic balls (Si_3N_4, Al_2O_3, Φ3 mm) were used as counterparts at a sliding frequency of 10 Hz and an amplitude of 1 mm. The film and the balls were ultrasonically cleaned in acetone prior to each friction testing. The friction testing was repeated four times for each sample. The worn surfaces of the carbon films and the balls were studied by using Raman spectroscopy and an optical microscope (Olympus STM6 Measuring Microscope), respectively.

3. Results and discussion

3.1. Microstructure and morphology

The cross-sectional structure of the graphite-like carbon film deposited at a bias of 125 V is shown in Fig. 2. It can be seen that the film has a bilayer structure. The upper layer is characterized by an amorphous and compact structure, which is a carbon film according to its thickness. The lower layer has a columnar structure owing to the crystal nature of the titanium and the titanium carbide. There is no distinct interface between the titanium and the titanium carbide layers.

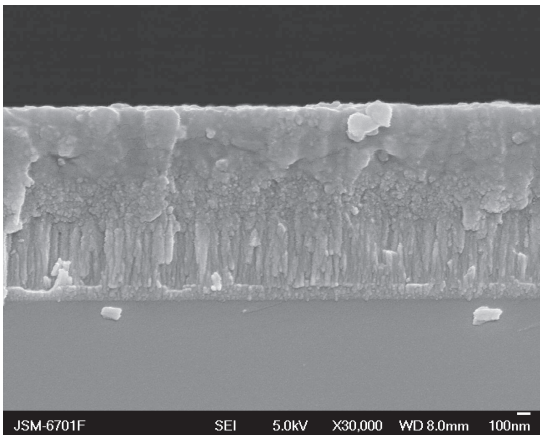


Fig. 2. FESEM image of graphite-like carbon film deposited at a bias voltage of 125 V.

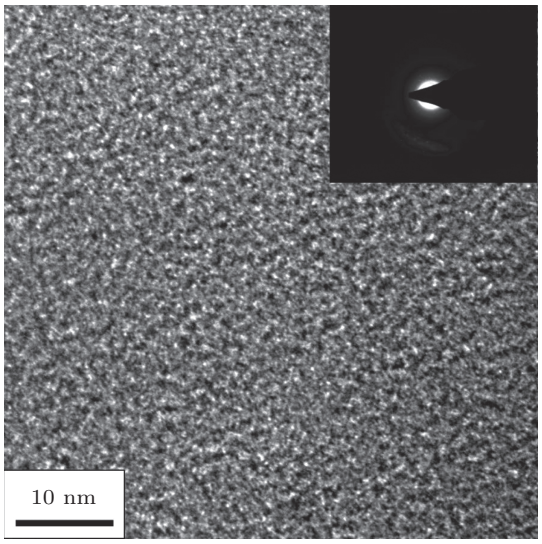


Fig. 3. HRTEM image of graphite-like carbon film deposited at a bias voltage of 125 V. The insert shows the corresponding SAED pattern.

Figure 3 demonstrates the HRTEM image and its corresponding selected area electron diffraction (SAED) pattern of the film deposited at a bias voltage of 125 V. As shown in Fig. 3, there is no crystal structure that can be directly observed from the image, indicating an amorphous structure of the present film, which is also confirmed by the SAED. The diffraction pattern does not show any obvious diffraction ring, demonstrating no crystalline structure existing in the film.

The surface morphologies of the films deposited at different bias voltages are investigated by using the atomic force microscope, and the corresponding images are shown in Fig. 4. It can be seen from Fig. 4 that each film surface is composed of many islands with different sizes. The film surface is relatively rough, but there is no obvious defect. The root mean square (RMS) roughness of the film is in the range from 5.0 nm to 7.5 nm, and is not obviously dependent on the deposition bias voltage. The roughness of the film is apparently higher than that of the diamond-like carbon film with a high sp^3 concentration.[8,9] The high surface roughness of the graphite-like carbon film originates mainly from the formation of a large number of sp^2 clusters during the deposition processes, which would substantially roughen the film by the surface diffusion to form a large number of islands with different sizes distributed randomly on the film surface.[10,11]

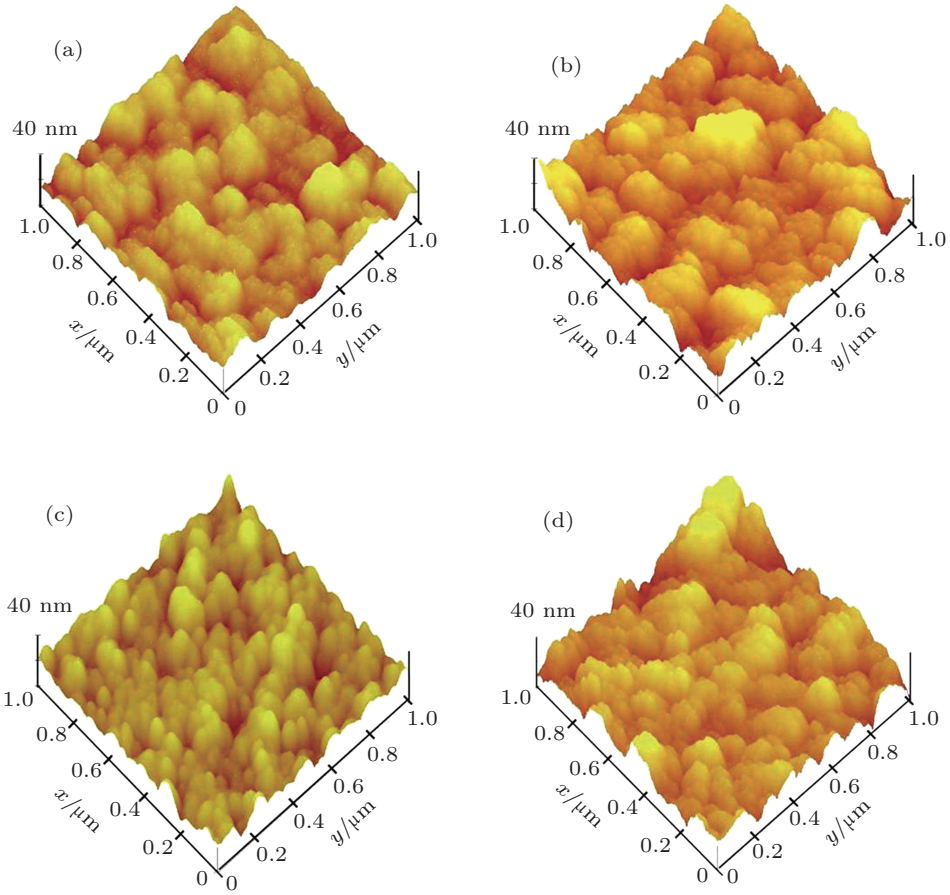


Fig. 4. (colour online) AFM images of graphite-like carbon films prepared under bias voltages of (a) 75 V, (b) 100 V, (c) 125 V, and (d) 150 V.

Visible Raman spectroscopy is used to investigate the microstructures of the carbon films, since this technique is very sensitive to the bonding structure of the sp^2 type, the cluster size, and the ordering inside the cluster. Figure 5 shows the Raman spectra of the graphite-like carbon films fabricated under different bias voltages. The spectra exhibit asymmetric broad Raman intensity distributions in the range from 900 cm^{-1} to 1800 cm^{-1} and centred around 1500 cm^{-1}, indicating a graphite-like characteristic.[6,12] In order to identify the peak positions, the Raman spectra are fitted by using two Gaussian line shapes. It is found that the asymmetric broad peak is made up of two peaks at $\sim$1370 cm^{-1} and $\sim$1570 cm^{-1}, which are the conventional D and G peaks originating from the different vibration modes of the sp^2 hybrid carbon, respectively.[13,14] The detailed fitting results for the Raman spectra of the resulting carbon films are illustrated in Table 1, including the positions, the full widths at half maximum (FWHMs), and the intensity ratios between the D and the G peaks (I_D/I_G), which would provide some important information about the film microstructure.[13,14]

Table 1 presents the detailed fitting parameters of the Raman spectra. It can be seen that the outstanding characteristics of the resulting films are the high intensity ratios between the D and the G peaks (> 4.0), which are one order of magnitude larger than that of the diamond-like carbon film reported in Ref. [15], indicating a more graphite-like structure. In addition, it can also be seen that with the deposition bias voltage increasing from 75 V to 150 V, the value of I_D/I_G decreases and reaches a minimum of 4.17 at 100 V, and then increases slightly and reaches

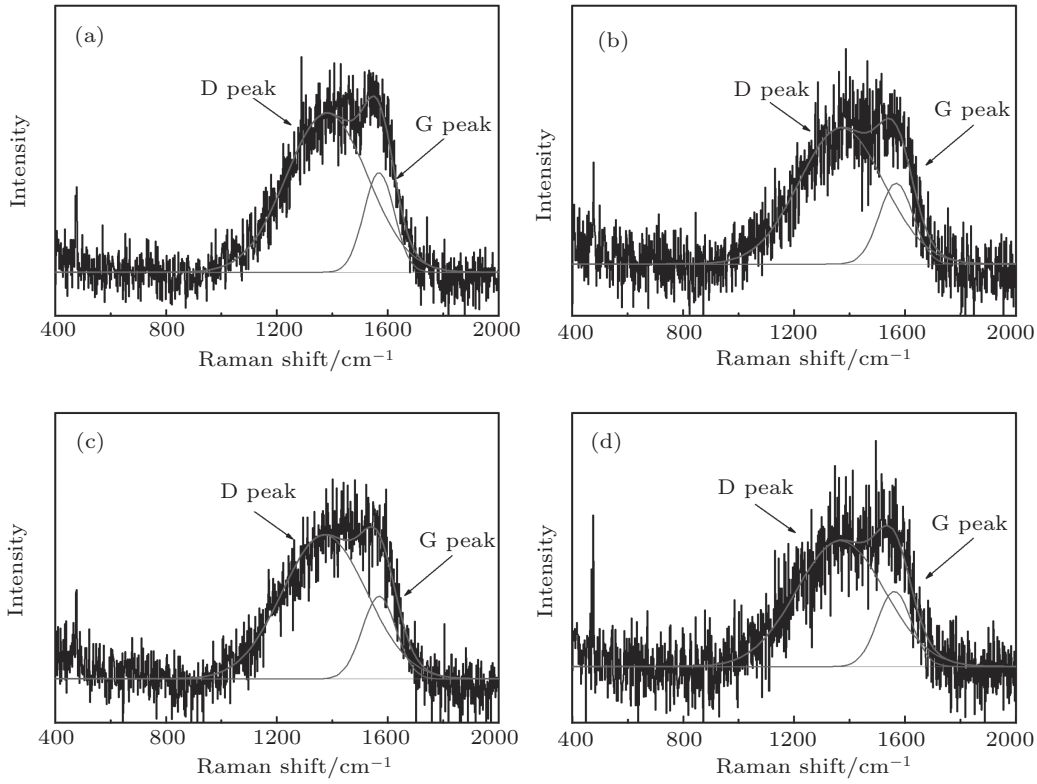


Fig. 5. Raman spectra of graphite-like carbon films deposited under bias voltages of (a) 75 V, (b) 100 V, (c) 125 V, and (d) 150 V.

Table 1. Fitting parameters for Raman spectra of graphite-like carbon films deposited under different bias voltages.

Bias/V	D peak/cm^{-1}	G peak/cm^{-1}	D FWHM/cm^{-1}	G FWHM/cm^{-1}	I_D/I_G
75	1380.72	1568.18	344.00	128.27	4.23
100	1370.64	1568.26	356.65	144.68	4.17
125	1371.62	1568.68	358.79	143.45	4.25
150	1371.08	1561.80	373.68	144.15	4.32

4.32 at 150 V. According to the variation trend of the intensity ratio between the D and the G peaks, it can be inferred that the sp^3 fraction in the film first increases and then decreases with the deposition bias voltage increasing. The FWHMs of the D and the G peaks of the present graphite-like carbon films are obviously broader than those of the amorphous carbon reported in Ref. [16], suggesting that a more disordered structure exists in the present film. The highly distorted structure of the film is favourable for improving its mechanical properties.[6]

3.2. Mechanical properties

Figure 6 exhibits the hardnesses and the internal stresses of the graphite-like amorphous carbon films deposited with different bias voltages. As can be seen, the deposition bias voltage has an obvious influence on the mechanical behaviour of the amorphous carbon film. The hardness of the amorphous carbon film starts from a value of 13.7 GPa under a deposition bias voltage of 75 V and then quickly increases to the maximum value of 17.5 GPa under the deposition bias voltage of 100 V. After that, the hardness monotonically decreases and reaches the minimum value of 12.1 GPa under the deposition bias voltage of 150 V. It is noticed that the maximum hardness of the graphite-like carbon film is obviously higher than that of the diamond-like carbon film in Refs. [8] and [9]. The previous studies have shown that the superior mechanical properties of the amorphous carbon films are usually ascribed to the presence of a high fraction of sp^3 sites in the films, whereas a high concentration of sp^2 sites is regarded as leading to the formation of a soft film.[17] However, the Raman spectra show that the present films each have an essentially graphitic-like structure with the presence of a high number of sp^2 bonds. Therefore, the formation mechanism of hardness for the graphite-like carbon film is obviously different from that for the diamond-like film. Recently, it has been shown that the amorphous carbon film with an onion-like structure has a large number of graphitic clusters in the structure,[18] and the film reveals superior mechanical properties, including high hardness and high elasticity. In that case, the high hardness is ascribed to the interlinking of the relatively separate graphitic clusters by the sp^3 bonds, which helps to improve the film hardness obviously. Likewise, the high hardness of the graphite-like carbon film could also be attributed to the intersecting of a large number of sp^2 clusters by the sp^3 bonds, which would improve the connectivity of the amorphous carbon network and hence increases the film hardness.[19] The variation trend of the film hardness with the deposition bias voltage is well consistent with that of the sp^3: sp^2 ratio obtained from the Raman analysis shown in Table 1, which can be well understood based on the fact that the sp^3 bonds play the role of interconnecting the separate graphitic clusters together. Therefore, the higher film hardness would be obtained for the film with a higher sp^3 content owing to the stronger crosslink effect.

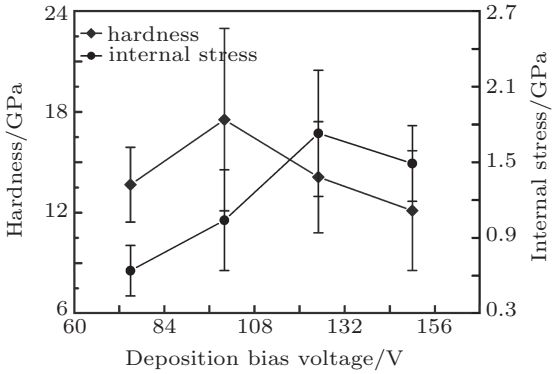


Fig. 6. Hardnesses and internal stresses of graphite-like carbon films prepared at various deposition bias voltages.

The high internal stress of the diamond-like carbon film greatly restricts its practical application, since it would cause the film to bulge and peel off from the substrate once it accumulates to a certain level during the deposition. Fortunately, the present graphite-like amorphous carbon films each have an internal stress as low as 0.64 GPa, which is favourable for obtaining high adhesion strength between the film and the substrate and achieving superior tribological properties in high load conditions.

3.3. Tribological properties

Figure 7 shows the average friction coefficients and the wear rates of the graphite-like carbon films deposited under different substrate bias voltages. It is obvious that the resulting graphite-like carbon films have superior tribological properties with a low friction coefficient (<0.06) and a low wear rate ($\sim 10^{-11}$ cm^3/Nm). What is interesting here is the high load bearing capacity of the graphite-like carbon films. The maximum Hertz contact stress is as high as 2.6 GPa, corresponding to a normal load of 20 N, which is obviously high than that of the diamond-like

carbon film reported in Ref. [20]. The friction coefficient does not change obviously with the increase of the deposition bias voltage. The wear decreases obviously with the increase of the deposition bias voltage, which may be due to the stronger adhesion strength in the interface originating from the increase in the intermixing effect at the higher deposition bias voltage.[21] The friction and the wear mechanism will be explained in more detail later.

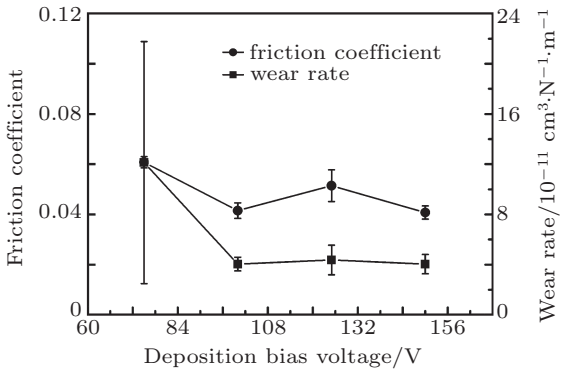


Fig. 7. Average friction coefficients and wear rates of graphite-like carbon films fabricated at different deposition bias voltages.

Figure 8 gives the tribological testing results for the film deposited at 125 V sliding against different counterpart balls (steel, Al_2O_3, Si_3N_4). It can be seen that when sliding against the steel ball, the graphite-like carbon film provides a relatively high friction coefficient ($\sim$0.05) and a high wear rate ($\sim$4.4 $\times$ 10^{-11} cm^3/Nm), while the friction coefficient and the wear rate for the case of the film sliding against the Si_3N_4 ball are relatively low, which are $\sim$0.04 and $\sim 3.4 \times 10^{-11}$ cm^3/Nm, respectively. The lowest friction coefficient and the lowest wear rate are obtained when the film slides against the Al_2O_3 ball, which are $\sim$0.03 and $\sim 3.1 \times 10^{-11}$ cm^3/Nm, respectively. Additionally, the friction coefficient curves are very stable in different cases, and the friction processes each have a very short run-in stage. Figure 8 also gives typical worn morphologies of the counterpart balls sliding against the carbon film. It is clearly shown that the different balls sustain different levels of abrasion, the steel ball suffers a very serious abrasion, the abrasion of the Al_2O_3 ball is relatively light. Meanwhile, a thick transfer layer is formed on each one of the steel balls, which is related to the superior tribological behaviours, as discussed later in this paper.

Figure 9 exhibits the Raman spectra inside and outside of the wear tracks after sliding against different balls. Different from the Raman spectra for our previous hydrogenated titanium containing diamond-like carbon films,[22] the Raman spectra inside and outside of the wear tracks for the graphite-like carbon films are very similar to each other, indicating no distinct graphitization occurred during the friction testing and a high thermal stability of the graphite-like carbon film.

Combining the above testing and characterization, we can conclude that the present graphite-like carbon films have superior tribological behaviours in atmosphere, which are even better than those of some

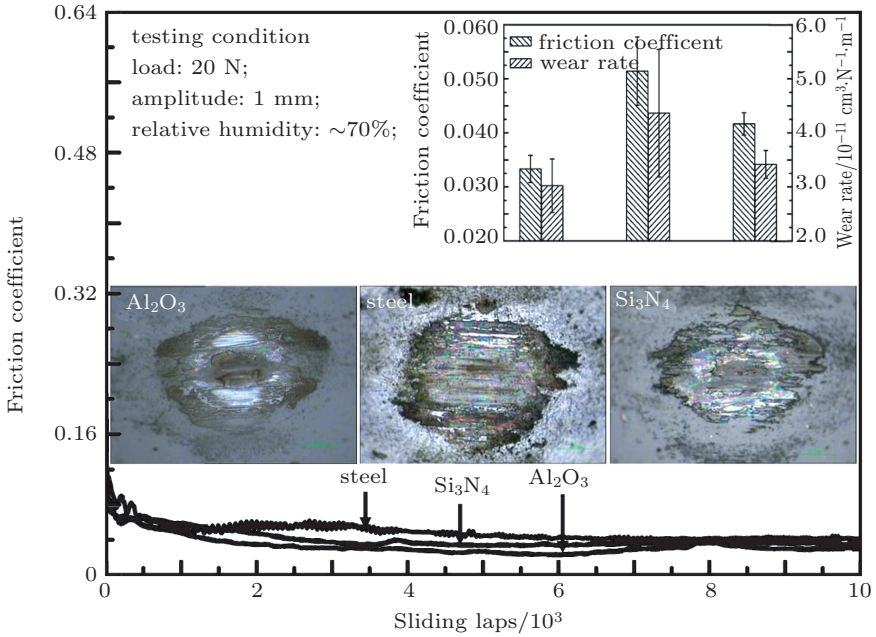


Fig. 8. (colour online) Tribological properties of graphite-like carbon films sliding against different balls. The insert shows the corresponding worn surface morphologies of the balls.

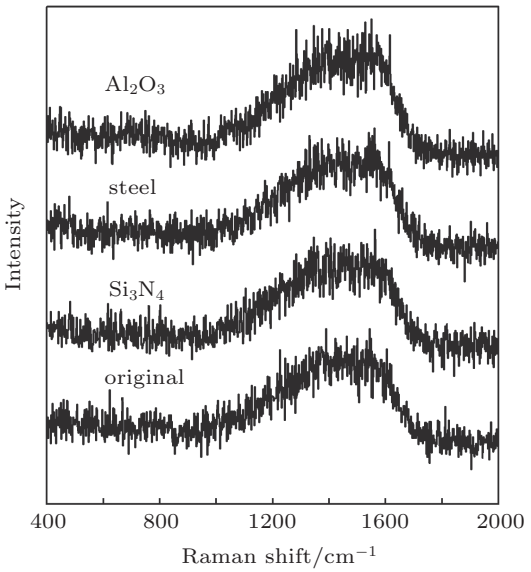


Fig. 9. Raman spectra of the original graphite-like carbon film surface and wear tracks of the film sliding against different balls.

high-quality diamond-like carbon films. The previous studies have shown that the film hardness plays an important role in determining the tribological property of the amorphous carbon film.[17] However, all the present graphite-like carbon films each have a moderately high hardness, no more than 20 GPa, which is only a typical value for the amorphous carbon film. Therefore, the superior tribological properties of the graphite-like carbon are related to other factors rather than the hardness. Firstly, the low internal stress of the graphite-like carbon film would provide the film with a high adhesion strength, which is favourable for achieving superior tribological properties for the carbon film, especially for the high load bearing capacity.[3] Secondly, the particular graphite-like structure would reduce the surface banding σ bonds effectively, therefore, the stronger interaction between the film surface and the ball would be diminished, and hence the low friction and wear are obtained. Thirdly, the formation of a thick transfer layer on the counterpart ball surface can prevent the direct contact between the carbon film and the ball surface and reduce the contact stress concentration on the film surface, helping to promote the wear resistance and the load bearing capacity further. Fourthly, for the diamond-like carbon films, especially for the hydrogenated ones, their thermal stability temperature limit can be easily reached in the typical tribological testing condition, which would affect the yield strength of the bulk material and degrade the tribological properties of the carbon films.[1,23] Fortunately, the good thermal stability of the graphite-like carbon film as indicated in Fig. 9 is favourable for maintaining the original superior wear resistance of the carbon film in the overall tribological period. Besides, the high relative humidity is propitious to obtain superior tribological properties for the present hydrogen-free amorphous carbon films by saturating the surface dangling bonds. The dependence of tribological property on the balls will be briefly discussed next.

The friction and the wear behaviours of the amorphous carbon film are determined by many factors, including carbon film properties, the counterpart material, testing conditions, etc. In our present case, special attention is paid to the study of the effect of the counterpart material on the tribological behaviour of the carbon film, and it is found that the tribological property of the carbon film is obviously dependent on the counter body. As shown in Fig. 8, the carbon film shows a better tribological property when it slides against the ceramic ball. It is well known that the ceramic ball is chemically more inert than the steel ball. When the steel ball slides against the carbon film in humid air, the interaction between the water molecules and the steel ball would accelerate the surface oxidation of the steel ball to form a large number of iron oxide abrasive particles during the friction process, leading to the high friction and wear for the friction pair. On the other hand, the contact stress would obviously influence the tribological behaviour. At a high contact stress, the friction and the wear would be reduced by converting more asperities and materials under the contact area into the thicker transfer layer.[24] At present, a higher contact stress is obtained with the ceramic balls owing to the high elastic modulus of the ceramic balls.

4. Conclusion

A series of graphite-like carbon films are successfully fabricated on the silicon substrates using the unbalanced magnetron sputtering. The Raman analysis shows that the resulting films are dominated by the sp^2 sites, and they have moderately high hardness, low internal stress, high surface roughness, and superior tribological behaviors. The deposition bias voltage has an obviously influence on the film structure and property. Namely, with the increase of the deposition bias voltage, the intensity ratio between the D and the G peaks first decreases and then increases, while the film hardness and the internal stress show

an inverse vibration trend, which first increases and then decreases. The resulting graphite-like carbon films show superior tribological properties in humid air with low friction, low wear, and high load bearing capacity, which are favourable for their applications in high load conditions.

References

[1] Neuville S and Matthews A 2007 *Thin Solid Films* **515** 6619

[2] Field S K, Jarratt M and Teer D G 2004 *Tribol. Int.* **37** 949

[3] Zeng X T, Zhang S, Ding X Z and Teer D G 2002 *Surf. Coat. Technol.* **420–421** 366

[4] Fu Y H, Zhu X D, He J W and Yang S C 2003 *Tribology* **23** 463 (in Chinese)

[5] Yan S P, Jiang B L, Su Y and Zhang Y H 2008 *Tribology* **28** 491 (in Chinese)

[6] Wang Y J, Li H X, Ji L, Zhao F, Liu X H, Kong Q H, Wang Y X, Quan W L, Zhou H D and Chen J M 2010 *J. Phys.* D: *Appl. Phys.* **43** 505401

[7] Zhao F, Li H X, Ji L, Mo Y F, Quan W L, Zhou H D and Chen J M 2009 *J. Phys.* D: *Appl. Phys.* **42** 165407

[8] Wang J, Liu G C, Wang L D, Deng X L and Xu J 2008 *Chin. Phys.* B **17** 3108

[9] Li H X, Xu T, Chen J M, Zhou H D and Liu H W 2005 *Acta Phys. Sin.* **54** 1885 (in Chinese)

[10] Peng X L, Barber Z H and Clyne T W 2001 *Surf. Coat. Technol.* **138** 23

[11] Lifshitz Y, Edrei R, Hoffman A, Grossman E, Lempert G D, Berthold J, Schultrich B and Jäger H U 2007 *Diamond Relat. Mater.* **16** 1771

[12] Konca E, Cheng Y T, Weiner A M, Dasch J M and Alpas A T 2006 *Surf. Coat. Technol.* **200** 3996

[13] Ferrari A C and Robertson J 2000 *Phys. Rev.* B **61** 14095

[14] Ferrari A C and Robertson J 2001 *Phys. Rev.* B **64** 075414

[15] Zhang Z Y, Lu X C, Luo J B, Shao T M, Qing T and Zhang C H 2006 *Chin. Phys.* **15** 2697

[16] Marcinauskas L, Valinčius V and Grigonis A 2011 *Surf. Coat. Technol.* **205** S71

[17] Robertson J 2002 *Mater. Sci. Eng.* R **37** 129

[18] Amaratunga G A J, Chhowalla M, Kiely C J, Alexandrou I, Aharonov R and Devenish R M 1996 *Nature* **383** 321

[19] Baptista D L and Zawislak F C 2004 *Diamond Relat. Mater.* **13** 1791

[20] Voevodin A A, Donley M S, Zabinski J S and Bultman J E 1995 *Surf. Coat. Technol.* **76–77** 534

[21] Liao J X, Liu W M, Xu T and Xue Q J 2004 *Carbon* **42** 387

[22] Zhao F, Li H X, Ji L, Wang Y J, Zhou H D and Chen J M 2010 *Diamond Relat. Mater.* **19** 342

[23] Neuville S 2002 *Diamond Relat. Mater.* **11** 1721

[24] Li R L, Tu J P, Hong C F, Liu D G, Zhou D H and Sun H L 2009 *J. Appl. Phys.* **106** 123508